

Journal of Basics and Applied Sciences Research (JOBASR) ISSN (print): 3026-9091, ISSN (online): 1597-9962

Volume 1(1) IPSCFUDMA 2025 Special Issue DOI: https://dx.doi.org/10.4314/jobasr.v1i1.8s



# Electronic and Optical Properties of Chalcone-Based Metal-Free Dyes with Naphthalene and Triphenylamine Donors: A TD-DFT Study

Hassan A.1\*

<sup>1</sup>Federal College of Education, Katsina

\*Corresponding Author Email: <a href="mailto:hassanabdulaziz30@gmail.com">hassanabdulaziz30@gmail.com</a>

#### **ABSTRACT**

This theoretical study demonstrates how donor substitution (Naphthalene vs. Triphenylamine) on cyanoacrylic acid as acceptor influences the optical absorption and charge transfer behavior of chalcone-based dyes, highlighting design strategies for improved dye-sensitized solar cells. Density functional theory (DFT) and time-dependent DFT (TD-DFT) at the B3LYP/6-311G (d,p) level were employed to optimize the geometries and analyze electronic and optical properties in DMF solvent using the IEFPCM model. The results show that both naphthalene dye (Ac 1) and triphenylamine dye (Ac 2) possess frontier molecular orbital (FMO) levels suitable for efficient electron injection into the TiO<sub>2</sub> conduction band and regeneration by the electrolyte. Ac 1 exhibited a higher absorption maximum (338 nm) due to extended conjugation in the naphthalene donor, while Ac 2 showed a narrower HOMO-LUMO gap (2.61 eV) and favorable HOMO alignment, supporting faster dye regeneration. Although Ac 1 benefits from stronger visible-light absorption, Ac 2 demonstrated better electronic coupling, which may enhance overall DSSC performance. Given their low fabrication cost, tunable molecular design, and compatibility with flexible substrates, such DSSCs hold great potential for practical applications in building-integrated photovoltaics and portable energy devices, offering a sustainable alternative to fossil-fuel-based energy sources.

## **Keywords:**

Dye Sensitized Solar Cell, Chalcone, Density Functional Theory (DFT), UV-Vis absorption, HOMO-LUMO.

### INTRODUCTION

The International Energy Agency (IEA) noted that global electricity demand is expected to rise significantly, driven by population growth and economic activities, particularly in emerging economies. Moreover, reducing heavy dependence on fossil fuels through decarbonization is essential to address pressing environmental concerns. As such, much emphasis is required for energy transitions to a cleaner and environmentally friendly energy derivation from renewable energy sources (solar). Renewable energy sources are sustainable and can be regarded to provide an endless source of energy. In recent years, a growing amount of important household demands such as electricity, air and water heating/cooling, transportation and rural (off-grid) energy services are being provided in many countries based on renewable energy sources(Sen et al., 2023). The share of renewables in electricity generation is forecast to rise from 30% in 2023 to 37% in 2026, with the growth largely supported by the expansion of ever cheaper solar PV (IEA, 2024). The most suitable way to resolve the global energy disaster is to utilize solar energy as renewable energy (Khan et al., 2023).

The main technologies that convert sunlight into electricity are solar cells. Among different solar cells,

dye-sensitized solar cell (DSSC) is suitable because of their amazing properties like simple manufacturing process, low cost, elasticity, environmentally friendly, and high efficiency (Mehmood et al., 2021; O'regan & Grätzel, 1991). Dye-sensitized solar cells (DSSCs) belong to the group of thin-film solar cells which have been under extensive research for more than two decades due to their low cost, simple preparation methodology, low toxicity and ease of production (Sharma et al., 2018). The performance of DSSCs is heavily influenced by the design and properties of the sensitizer dye, which plays a crucial role in light absorption and electron injection semiconductor. Metal-based complex dyes and metalfree organic dyes are the two main classes of DSSCs (Sen et al., 2023). Over the past two decades, the metal-free organic dyes have been proposed due to several advantages over organometallic dyes(Jiang et al., 2014; Nachimuthu et al., 2014, 2016; Santhanamoorthi et al., 2013; Tseng et al., 2014). Metal-free organic dyes utilize organic molecules as sensitizers, often composed of conjugated  $\pi$ -systems (Ferdowsi et al., 2020; Lin et al., 2020).

Chalcone is one of the metal-free organic dyes that

shows promising behavior in photonics applications especially DSSC. Chalcone-based dyes have emerged as a versatile class of organic sensitizers for dve-sensitized solar cells (DSSCs) due to their tunable optical properties, facile synthesis, and structural diversity (Mohd Nizar et al., 2021). The efficiency of chalcone dyes in DSSCs can significantly enhanced by the strategic substitution/modification of substituents on the chalcone backbone. Substituents, particularly electron-donating and electron-withdrawing groups, impact key parameters such as light absorption, charge transfer efficiency, and interaction with the semiconductor surface.

Ouantum chemical methods have been employed in recent decades as a sustainable approach for elucidating the relationship between molecular geometries and dye characteristics, thus offering a reliable theoretical platform for the rapid screening of efficient dyes before expensive and time-consuming syntheses (Rashid et al., 2020). Density functional theory (DFT) and timedependent density functional theory (TDDFT) have been extensively used to investigate the electronic and optical properties of virtual photosensitizers in the ground and excited states for the development of DSSCs(Adamo et al., 2012; Martsinovich & Troisi, 2011). Therefore, the theoretical predictions based on DFT calculations are promising, as they correlate well with the experimental data on DSSCs (Al-Eid et al., 2014). The substitution of cyano group together with a carboxylic acid in the anchoring part of organic dyes has been more popular in recent years (Hara et al., 2003; Ma et al., 2014; Manzhos et al., 2012; Pastore & De Angelis, 2012). Despite promising reports, the effect of specific donor substitutions (naphthalene vs. TPA) in chalcone-based dyes remains underexplored.

Thus, this study aims to theoretically investigate the effect of Naphthalene and Triphenylamine (TPA) as donors for chalcone dyes Ac 1 and Ac 2, respectively, while both of them utilize cyanoacrylic acid as an acceptor in enhancing the overall DSSC performance. Understanding these effects will contribute to the development of highly efficient chalcone-based sensitizers for next-generation DSSCs. The findings will pave the ways to synthesizing chalcone compounds with robust character in DSSC, which translates to fostering sustainable technology and innovation for affordable, clean, and environmentally friendly energy derivation that can combat climate change. It will help policymakers develop renewable

energy policies, expand energy access, and create economic opportunities while supporting environmental sustainability and reducing carbon footprints.

#### MATERIALS AND METHODS

### **Computational Methods**

All quantum chemical calculations were performed using density functional theory (DFT) with the B3LYP functional, which combines Becke's three-parameter exchange (Becke, 1993) and the Lee-Yang-Parr correlation (LYP). The polarized split-valence basis set 6-311G (d,p) was employed to achieve a balance between computational cost and accuracy. Initial molecular geometries were constructed and preoptimized in Avogadro (Hanwell et al., 2012), followed by full geometry optimizations without symmetry constraints. The frequency calculations were performed to confirm the stationary nature of the optimized geometries at energy minimum using the same level of theory. The absence of imaginary frequencies confirms that all the dyes are optimized at minimum ground state energy(Unny et al., 2018). Time-dependent DFT (TD-DFT) calculations at the same level of theory were carried out on the optimized geometries to obtain vertical excitation energies, oscillator strengths, and simulated UV-Vis absorption effects were modeled Solvent dimethylformamide (DMF) using the integral equation formalism of the polarizable continuum model (IEFPCM) within the self-consistent reaction field (SCRF) approach, to better mimic the DSSC environment. All computations were performed with the Gaussian 09 software package (Frisch et al., 2009).

### RESULTS AND DISCUSSION

# **Ground state geometry**

The molecular structures of the designed chalcone derivatives were fully optimized in their ground state without any symmetry constraints using hybrid density functional theory with 6-311(d,p) basis set. All the parameters were fully allowed to relax and each of the calculations converged to an optimized geometry which corresponds to a true energy minimum (Abdulaziz et al., 2019).

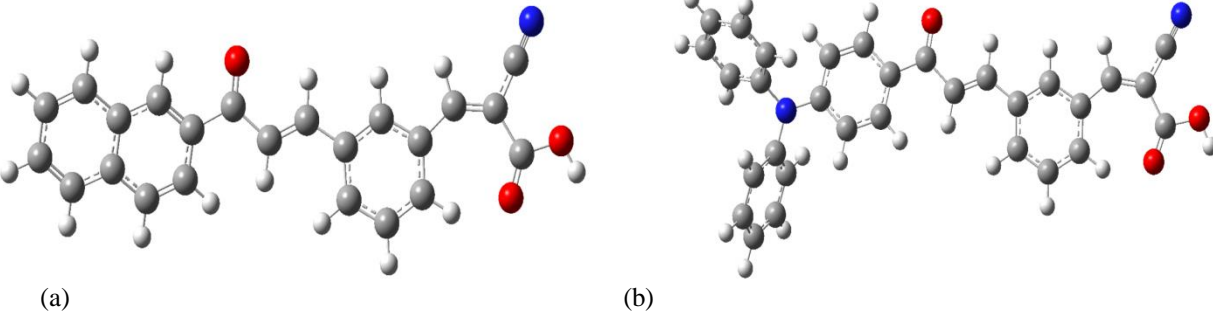


Fig 1. Optimized geometries of (a) Ac 1 and (b) Ac 2 chalcone derivatives.

The optimized geometrical parameters (**Table 1**), including bond lengths, bond angles, and dihedral angles, were analyzed to evaluate planarity and electronic delocalization across the conjugated framework. Understanding the structural characteristics of these compounds is imperative for optimizing their electron injections (Dulo et al., 2021; Luan et al., 2013). In general, A molecule with a short bond distances and small bond angles that exist between its substituent atoms is expected to be stronger than one with a long bond distances and a large bond angle (Abdulaziz et al., 2019). Both Ac 1 and Ac 2 show comparable bond lengths and angles, with a typical enone C=C bond length of 1.34 Å shorter than the C-C single bond (1.49 Å), reflecting  $\pi$ -electron delocalization.

The dihedral angles affect the overlap of molecular orbitals, impacting electronic coupling(Nassar et al.,

2024). The dihedral angle in Ac 1 between the enone bridge and the naphthalene donor (C7–C8–C11–C13 = 166.40°) indicates a slight twist that does not significantly disrupt overall planarity. In contrast, the triphenylamine (TPA) moiety in Ac 2 exhibits pronounced non-planarity, as its three phenyl rings surrounding the nitrogen core adopt nearly perpendicular orientations (twisted) relative to each other and to the enone bridge unlike the more planar naphthalene donor in Ac 1. Only the immediate phenyl ring connected to the enone maintains near planarity  $(C27-C28-C34-C36 = -172.18^{\circ})$ . This conformational distortion in Ac 2 reduces direct intramolecular charge transfer across the TPA unit, but helps suppress dye aggregation, while the phenyl ring aligned with the  $\pi$ system maintains effective donor-acceptor conjugation.

**Table 1:** Selected bond length in angstroms (A°), bond angles, and dihedral angles in degree (°) of the optimized dves obtained at B3LYP/6-311G (d,p) level of theory in gas phase.

Ac 1		Ac 1		
Bond	Length	Bond	Length	
C11-O12	1.22	C34-C35	1.22	
C11-C13	1.49	C34-C36	1.49	
C13-C30	1.34	C36-C37	1.34	
C30-C29	1.46	C37-C41	1.46	
C25-C26	1.46	C43-C47	1.46	
C25-C35	1.37	C47-C48	1.37	
C34-C35	1.49	C48-C50	1.49	
C35-C36	1.44	C48-C49	1.43	
C36-N37	1.16	C49-N54	1.16	
C34-O40	1.35	C50-O51	1.35	
C34-O41	1.21	C50-O53	1.21	
Bond	Angle	Bond	Angle	
C25-C35-C36	115.62	C47-C48-C49	115.62	
C34-C35-C36	115.77	C50-C48-C49	115.78	
C25-C35-C34	128.61	C47-C48-C50	128.60	
C35-C34-O41	127.03	C48-C50-O53	127.07	
O40-C34-O41	121.99	O51-C50-O53	121.94	
C34-O40-H42	106.71	C50-O51-H52	106.67	•
C26-C25-C35	137.29	C43-C47-C48	137.30	•
C35-C36-N37	177.99	C48-C49-N54	178.00	•

Bond	Dihedral	Bond	Dihedral
C8-C13-C30-C29	-176.45	C28-C36-C37-C41	178.21
C7-C8-C11-C13	166.40	C27-C28-C34-C36	-172.18
C13-C30-C29-C28	176.97	C36-C37-C41-C42	-178.19
C28-C26-C25-C35	-179.16	C42-C43-C47-C48	179.27
C25-C35-C34-O41	-0.46	C47-C48-C50-O53	0.54
C36-C35-C34-O40	-0.32	C49-C48-C50-O51	0.43
C36-C35-C34-O41	179.70	C49-C48-C50-O53	-179.57
C35-C34-O40-H42	-0.01	C48-C50-51-H52	-179.99
O41-C34-O40-H42	-0.03	O53-C50-O51-H52	0.007

The dihedral angles along the cyanoacrylic acid acceptor group are all close to  $0^{\circ}$  or  $180^{\circ}$ , indicating that the cyanoacrylic acid moiety adopts a nearly planar conformation. This planarity facilitates extensive  $\pi$ -conjugation from the donor unit through the enone bridge to the electron-withdrawing –CN and –COOH groups. Such geometry enhances intramolecular charge transfer and is expected to improve electron injection into the  $TiO_2$  conduction band, while also favoring strong dye anchoring via the COOH group. Cyanoacrylic acid is the most commonly studied acceptor and it is the best acceptor till date since it is forming a strong ester linkage with  $TiO_2$  surface, which provides a path for electron injection from dye to the conduction band (CB) of  $TiO_2$  surface (Kim et al., 2013; Wan et al., 2012).

# Linear absorption studies

Linear absorption studies were performed using time-dependent DFT calculated in DMF solvent to simulate the electronic excitation behavior of Ac~1 and Ac~2. The UV-Vis absorption spectra are depicted in Fig. 2. The objective of this methodology was to clarify the role of molecular orbitals in electronic transmissions, resulting in the derivation of essential parameters including maximum absorption ( $\lambda_{max}$ ), excitation energies ( $E_{ex}$ ), oscillator strength (f), and major contribution (Nassar et al., 2024). These studies are crucial for interpreting optical properties, especially in the context of electronic excitations, although it is based on the theoretical predictions.

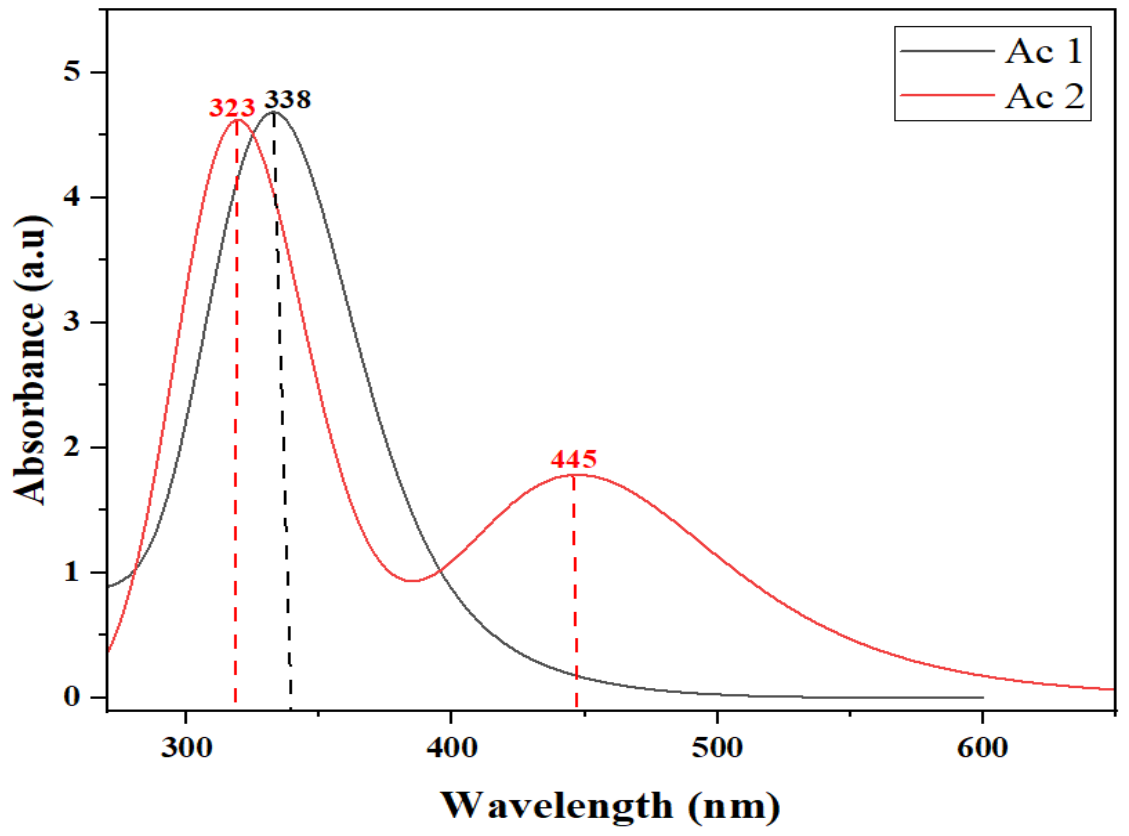


Fig. 2. UV-Vis absorption spectra of Ac 1 (grey solid line) and Ac 2 (red solid line) calculated in DMF using

B3LYP/6-311G(d,p)) basis set.

It is observed that Ac 1 and Ac 2 absorbed at 338 and 323nm respectively, this intense absorption bands with the maximum intensity towards the visible region (K band) are originated owing to the  $\pi \to \pi^*$  transitions (Maidur et al., 2025). Compounds that specifically contain a triphenylamine (TPA) unit as a donor end-unit were shown to exhibit an intense and broad absorption band that extended from UV to the far-red end of the visible spectrum. Their absorption spectra displayed a broad transition band that extended from 400 to 800 nm (D'Aléo et al., 2012). As a result, the 445nm broad absorption observed in Ac 2 (less intense R band) spectra is attributed to the n  $\rightarrow$   $\pi^*$  transitions where the nonbonding electrons absorb the UV radiations at lower energy levels than  $\pi$  to  $\pi^*$  transitions because they involve promoting an electron from a non-bonding orbital rather than a bonding one. This is due to the lone pair electron from the hetero-nitrogen atom in the TPA (donor chromophores). The intense experimental absorption bands of TPA-substituted chalcones were observed to peaked between 381 and 435 nm (Soc et al., 2019). This

corresponds to the  $\pi \to \pi$  transition at 323 nm and the  $n \rightarrow \pi$  transition at 445 nm observed in this study. The bathochromic-shifted absorption of Ac 1 (338 nm) compared to Ac 2 (323 nm) is primarily attributed to the enhanced planarity and extended conjugation of the naphthalene donor, which facilitates stronger intramolecular charge transfer to the cyanoacrylic acid acceptor. In contrast, the twisted geometry of the TPA donor in Ac 2 disrupts  $\pi$ -conjugation and leads to a blue-shifted absorption. The higher value of absorption wavelength is directly related to the electron donating ability of the donor moieties which is accounted for rigidity as well as planarity of the moiety which is evident from the dihedral angle measurement of the optimized dye structures (Unny et al., 2018). However, the absorption wavelengths of both compounds determine their eligibility to be part of the vital components in DSSC. Table 2 contains the detailed description of these absorption parameters of both compounds.

**Table 2:** Absorption spectral data calculated at TD-DFT/B3LYP/6-311G(d,p) level

Dye	λ <sub>max</sub> (nm)	E (eV)	$\overline{f}$	State Assi	ignment ]	Major Contribution
Ac 1	337.84	3.6699	1.2298	$S_0 - S_5$	H−1 → L-	+1 0.60111 (72.27%)
	320.98	3.8626	0.1401	$S_0 - S_6$	$H-2 \rightarrow L$	0.49014 (48.05 %)
	319.58	3.8795	0.5050	$S_0 - S_7$	$H-3 \rightarrow L$	0.46831 (43.86%)
Ac 2	445.45	2.7833	0.6752	$S_0 - S_2$	$H \rightarrow L+1$	0.69918(97.77%)
	323.17	3.8365	0.9870	$S_0 - S_5$	$H-1 \rightarrow L+$	-1 0.45093 (40.67%)
	321.56	3.8557	0.2719	$S_0 - S_6$	$H-3 \rightarrow L$	0.42308 (35.79%)

<sup>\*</sup>H=HOMO, L=LUMO

## The frontier molecular orbitals

The frontier molecular orbitals of Ac 1 and Ac 2 dyes (Fig. 2), are important criteria for determining intramolecular charge transfer (ICT) within an organic compound, which is a primary characteristic that depict a dye's ability to participate in an organic solar cell. In the orbital plots green phase indicates a positive phase, while the red phase indicates a negative phase. Considering both dyes, it is observed that electron densities of the HOMO are delocalized around the naphthalene and TPA (donor region) in Ac 1 and Ac 2 respectively which is extended

up to the carbonyl moiety, while the electron densities of the LUMOs were mainly delocalized from the carbonyl group along the enone bridge to the cyanoacrylic acid moiety (acceptor region) in both dyes. This was beneficial for the photon-driven ICT process and led to a charge transfer from the donor to the acceptor. ICT is facilitated if the electron density distribution of the HOMO is located near the electron donor, while that of the LUMO is delocalized around an anchoring group, ready for electron injection into the CB of the titanium oxide (TiO<sub>2</sub>) semiconductor (Rashid et al., 2020).

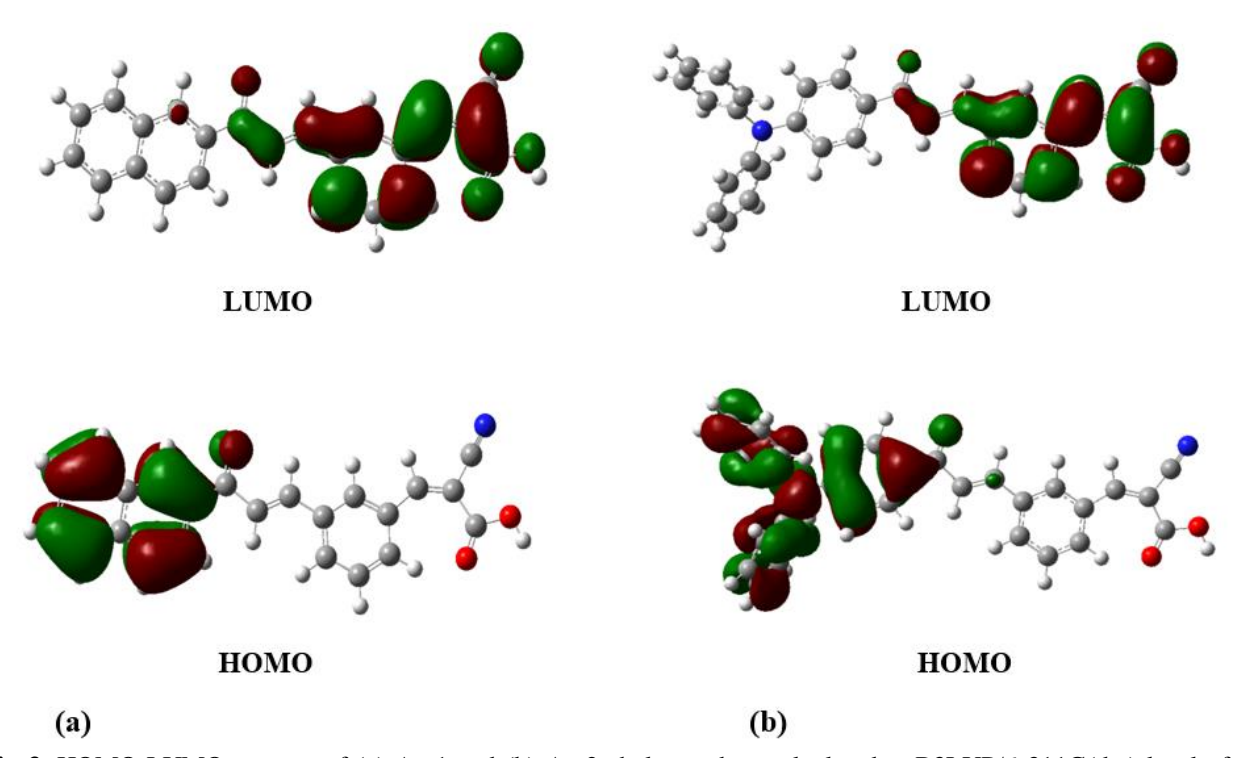


Fig 3. HOMO-LUMO contour of (a) Ac 1 and (b) Ac 2 chalcone dyes calculated at B3LYP/6-311G(d,p) level of theory.

The substituted naphthalene and TPA at the donor side of both dyes are  $\pi$ -rich systems, capable of donating electrons into the conjugated bridge,  $\alpha,\beta$ -unsaturated carbonyl bridge which serves as a  $\pi$ -linker that connects donor and acceptor via the conjugated path, it enables intramolecular charge transfer whereas the presence of a

strong acceptor cyanoacrylic acid at the anchoring side is for the cyano group to facilitate electron withdrawing process, as it is electron-deficient due to the electronegative nature of nitrogen atom and the carboxylic acid to facilitate the anchoring to the semiconductor.

**Table 3**: HOMOs, LUMOs and corresponding energy gap of the **Ac 1** & **Ac 2** dye molecules were implemented by using B3LYP/6-31G(d) basis set

DYE	λ (nm)	НОМО	LUMO	E <sub>g</sub> (eV)	
Ac 1	338	-6.38	-3.08	3.30	
Ac 2	323	-5.59	-2.98	2.61	

**Table 3** shows the HOMO and LUMO energies of the two dyes and the energy gap that exists between them. **Ac 2** has a higher HOMO energy (-5.59 eV) than **Ac 1** (-6.38 eV), which is consistent with triphenylamine's stronger electron-donating ability. The LUMOs are relatively close, but **Ac 1** has a slightly more stabilized LUMO. Although **Ac 2** exhibits a narrower HOMO–LUMO gap

of 2.61 eV due to the strong electron-donating ability of TPA, its twisted geometry limits effective conjugation across the donor– $\pi$ –acceptor system. As a result, **Ac 1**, with its more planar and rigid naphthalene donor, shows a red-shifted maximum absorption wavelength (338 nm), indicating more efficient  $\pi$ -electron delocalization and better donor–acceptor interaction.

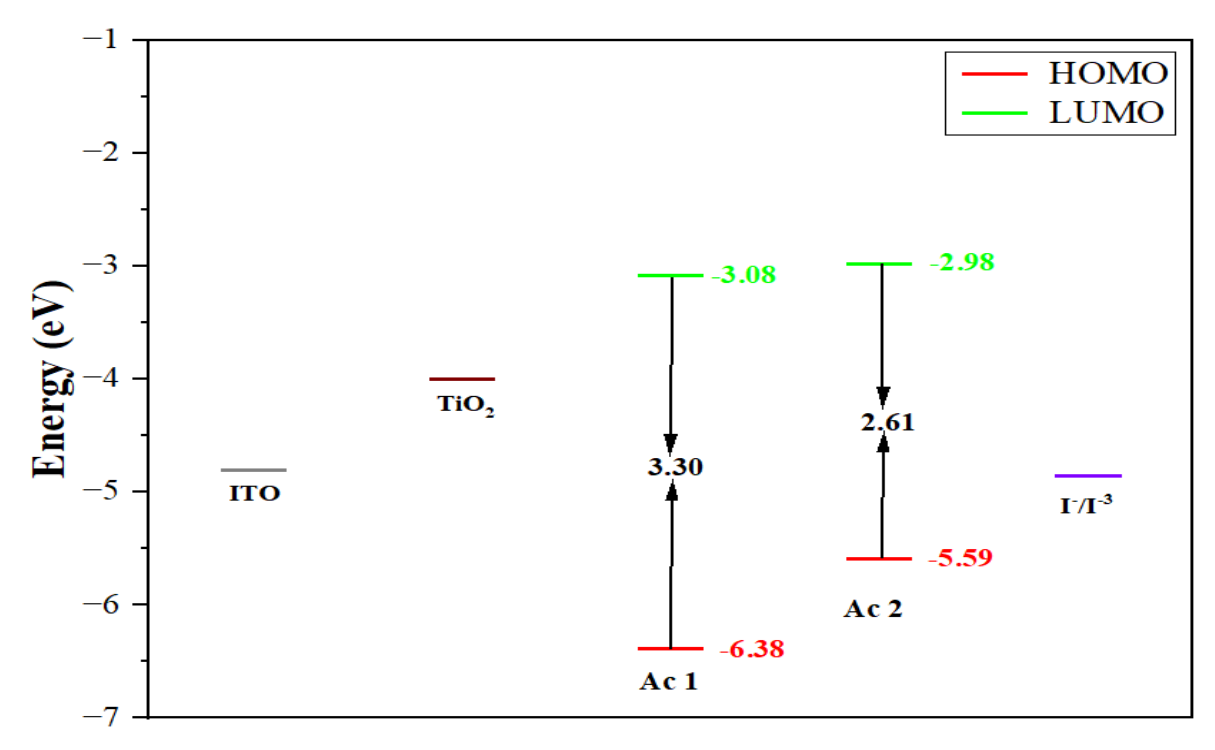


Fig. 4. The calculated energy alignment diagram of Ac 1 & Ac 2 based on DFT

The energy alignment diagram (Fig. 4) illustrates the relative positioning of the HOMO and LUMO energy levels of the two dyes with respect to the conduction band of TiO<sub>2</sub> and the redox potential of the electrolyte. Both dyes exhibit favorable alignment, with the LUMO levels positioned above the conduction band of TiO<sub>2</sub>, facilitating efficient electron injection, and the HOMO levels situated below the redox potential, ensuring effective dye regeneration. Notably, Ac 2 exhibits a HOMO level that lies closer to the redox potential compared with that of the Ac 1, which is advantageous for rapid electron replenishment by the redox mediator. Additionally, its narrower energy gap promotes easier excitation of electrons to the LUMO, thereby enhancing electron transfer to the semiconductor. These features suggest that Ac 2 may possess superior electronic coupling characteristics, potentially leading to improved dyesensitized solar cell (DSSC) performance.

#### **CONCLUSION**

This study investigated the influence of Naphthalene (Ac 1) and Triphenylamine (Ac 2) donors on chalcone-based dyes using DFT and TD-DFT. Ac 1 exhibited stronger light harvesting due to extended  $\pi$ -conjugation, while Ac 2 showed a narrower energy gap (2.61 eV) and better HOMO–redox alignment. These features suggest that Ac 1 favors visible light absorption, whereas Ac 2 may offer superior charge regeneration and electronic coupling. Overall, the results underscore the importance of donor engineering in optimizing DSSC performance.

#### REFERENCES

Abdulaziz, H., Gidado, A. S., Musa, A., & Lawal, A. (2019). Electronic Structure and Non-Linear Optical Properties of Neutral and Ionic Pyrene and Its Derivatives Based on Density Functional Theory. *Journal of Materials Science Research and Reviews*, 2(1), 91–103.

https://doi.org/10.9734/jmsrr/2019/v2i136

Adamo, C., Labat, F., Le Bahers, T., Ciofini, I., & Adamo, C. (2012). Solar Cells: Challenges and Perspectives. *Acc. Chem. Res.*, 45(8), 1268–1277.

Al-Eid, M., Lim, S., Park, K. W., Fitzpatrick, B., Han, C. H., Kwak, K., Hong, J., & Cooke, G. (2014). Facile synthesis of metal-free organic dyes featuring a thienylethynyl spacer for dye sensitized solar cells. *Dyes and Pigments*, *104*, 197–203. https://doi.org/10.1016/j.dyepig.2014.01.004

D'Aléo, A., Gachet, D., Heresanu, V., Giorgi, M., & Fages, F. (2012). Efficient NIR-light emission from solid-state complexes of boron difluoride with 2'-hydroxychalcone derivatives. *Chemistry - A European Journal*, 18(40), 12764–12772. https://doi.org/10.1002/chem.201201812

Dulo, B., Phan, K., Githaiga, J., Raes, K., & De Meester, S. (2021). Natural quinone dyes: A review on structure, extraction techniques, analysis and

application potential. Waste and Biomass Valorization, 12(12), 6339–6374.

Ferdowsi, P., Saygili, Y., Jazaeri, F., Edvinsson, T., Mokhtari, J., Zakeeruddin, S. M., Liu, Y., Grätzel, M., & Hagfeldt, A. (2020). Molecular engineering of simple metal-free organic dyes derived from triphenylamine for dye-sensitized solar cell applications. *ChemSusChem*, *13*(1), 212–220.

Frisch, M. J., Trucks, G. W., Schlegel, H. B., Scuseria, G. E., Robb, M. A., Cheeseman, J. R., Scalmani, G., Barone, V., Petersson, G. A., Nakatsuji, H., Li, X., Caricato, M., Marenich, A., Bloino, J., Janesko, B. G., Gomperts, R., Mennucci, B., Hratchian, H. P., Ortiz, J. V., Izmaylov, A. F., Sonnenberg, J. L., Williams-Young, D., Ding, F., Lipparini, F., Egidi, F., Goings, J., Peng, B., Petrone, A., Henderson, T., Ranasinghe, D., Zakrzewski, V. G., Gao, J., Rega, N., Zheng, G., Liang, W., Hada, M., Ehara, M., Toyota, K., Fukuda, R., Hasegawa, J., Ishida, M., Nakajima, T., Honda, Y., Kitao, O., Nakai, H., Vreven, T., Throssell, K., Montgomery, J. A., Peralta, J. E., Ogliaro, F., Bearpark, M., Heyd, J. J., Brothers, E., Kudin, K. N., Staroverov, V. N., Keith, T., Kobayashi, R., Normand, J., Raghavachari, K., Rendell, A., Burant, J. C., Iyengar, S. S., Tomasi, J., Cossi, M., Millam, J. M., Klene, M., Adamo, C., Cammi, R., Ochterski, J. W., Martin, R. L., Morokuma, K., Farkas, O., Foresman, J. B., & Fox, D. J. (2016). Gaussian 09, Revision A.02. Gaussian, Inc., Wallingford CT.

Hanwell, M. D., Curtis, D. E., Lonie, D. C., Vandermeersch, T., Zurek, E., & Hutchison, G. R. (2012). Avogadro: an advanced semantic chemical editor, visualization, and analysis platform. *Journal of Cheminformatics*, *4*(1), 17. https://doi.org/10.1186/1758-2946-4-17

Hara, K., Sato, T., Katoh, R., Furube, A., Ohga, Y., Shinpo, A., Suga, S., Sayama, K., Sugihara, H., & Arakawa, H. (2003). Molecular design of coumarin dyes for efficient dye-sensitized solar cells. *The Journal of Physical Chemistry B*, 107(2), 597–606.

IEA. (2024). Electricity 2024: Analysis and forecast to 2026. *IEA Publications*, 1–170. https://www.iea.org/news/global-coal-demand-expected-to-decline-in-coming-years

Jiang, S., Fan, S., Lu, X., Zhou, G., & Wang, Z.-S. (2014). Double D– $\pi$ –A branched organic dye isomers for dye-sensitized solar cells. *Journal of Materials Chemistry A*, 2(40), 17153–17164.

Khan, M. I., Mumtaz, S., Mustafa, G. M., Amami, M., Shahzad, U., & Al-Abbad, E. A. (2023). Improving the

current density and reducing the recombination rate of dye sensitized solar cells by modifying the band gap of Titania using Novel heterostructures. *Optical Materials*, 140, 113780. https://doi.org/https://doi.org/10.1016/j.optmat.2023.11 3780

Kim, B. G., Chung, K., & Kim, J. (2013). Molecular design principle of all-organic dyes for dye-sensitized solar cells. *Chemistry - A European Journal*, *19*(17), 5220–5230. https://doi.org/10.1002/chem.201204343

Lin, F.-S., Priyanka, P., Fan, M.-S., Vegiraju, S., Ni, J.-S., Wu, Y.-C., Li, Y.-H., Lee, G.-H., Ezhumalai, Y., & Jeng, R.-J. (2020). Metal-free efficient dye-sensitized solar cells based on thioalkylated bithiophenyl organic dyes. *Journal of Materials Chemistry C*, 8(43), 15322–15330.

Luan, F., Xu, X., Liu, H., & Cordeiro, M. N. D. S. (2013). Review of quantitative structure-activity/property relationship studies of dyes: recent advances and perspectives. *Coloration Technology*, *129*(3), 173–186.

Ma, J.-G., Zhang, C.-R., Gong, J.-J., Yang, B., Zhang, H.-M., Wang, W., Wu, Y.-Z., Chen, Y.-H., & Chen, H.-S. (2014). The adsorption of  $\alpha$ -cyanoacrylic acid on anatase TiO2 (101) and (001) surfaces: A density functional theory study. *The Journal of Chemical Physics*, 141(23).

Maidur, S. R., Ekbote, A. N., Patil, P. S., Katturi, N. K., Venugopal Rao, S., Wong, Q. A., & Quah, C. K. (2025).Structural and ultrafast third-order nonlinearities of methyl and methoxy substituted anthracene chalcones: Z-scan, four-wave mixing, and DFT approaches. Spectrochimica Acta - Part A: Molecular Biomolecular Spectroscopy, and 325(September 2024), 125146. https://doi.org/10.1016/j.saa.2024.125146

Manzhos, S., Segawa, H., & Yamashita, K. (2012). The effect of ligand substitution and water coadsorption on the adsorption dynamics and energy level matching of amino-phenyl acid dyes on TiO 2. *Physical Chemistry Chemical Physics*, 14(5), 1749–1755.

Martsinovich, N., & Troisi, A. (2011). Theoretical studies of dye-sensitised solar cells: From electronic structure to elementary processes. *Energy and Environmental Science*, *4*(11), 4473–4495. https://doi.org/10.1039/c1ee01906f

Mehmood, B., Khan, M. I., Iqbal, M., Mahmood, A., &

Al-Masry, W. (2021). Structural and optical properties of Ti and Cu co-doped ZnO thin films for photovoltaic applications of dye sensitized solar cells. *International Journal of Energy Research*, 45(2), 2445–2459.

Mohd Nizar, S. N. A., Ab Rahman, S. N. F., Zaini, M. F., Anizaim, A. H., Abdul Razak, I., & Arshad, S. (2021). The Photovoltaic Performance of Sensitizers for Organic Solar Cells Containing Fluorinated Chalcones with Different Halogen Substituents. *Crystals*, *11*(11), 1357.

Nachimuthu, S., Chen, W.-C., Leggesse, E. G., & Jiang, J.-C. (2016). First principles study of organic sensitizers for dye sensitized solar cells: effects of anchoring groups on optoelectronic properties and dye aggregation. *Physical Chemistry Chemical Physics*, 18(2), 1071–1081.

Nachimuthu, S., Lai, K.-H., Taufany, F., & Jiang, J.-C. (2014). Theoretical study on molecular design and optical properties of organic sensitizers. *Physical Chemistry Chemical Physics*, *16*(29), 15389–15399.

Nassar, M. F., Abdulmalek, E., Ismail, M. F., & Ahmad, S. A. A. (2024). Enhancing the performance of pyridyl carboxamide-N,N-dimethyl amino chalcone (PCC) as a dye sensitizer for dye-sensitized solar cells (DSSCs) through the incorporation of electron donor moieties. *International Journal of Electrochemical Science*, 19(9), 100715. https://doi.org/10.1016/j.ijoes.2024.100715

O'regan, B., & Grätzel, M. (1991). A low-cost, high-efficiency solar cell based on dye-sensitized colloidal TiO2 films. *Nature*, *353*(6346), 737–740.

Pastore, M., & De Angelis, F. (2012). Computational modelling of TiO 2 surfaces sensitized by organic dyes with different anchoring groups: adsorption modes, electronic structure and implication for electron injection/recombination. *Physical Chemistry Chemical Physics*, 14(2), 920–928.

Rashid, M. A. M., Hayati, D., Kwak, K., & Hong, J. (2020). Theoretical investigation of azobenzene-based photochromic dyes for dye-sensitized solar cells. *Nanomaterials*, *10*(5). https://doi.org/10.3390/nano10050914

Santhanamoorthi, N., Lai, K.-H., Taufany, F., & Jiang, J.-C. (2013). Theoretical investigations of metal-free dyes for solar cells: Effects of electron donor and acceptor groups on sensitizers. *Journal of Power Sources*, 242, 464–471.

Sen, A., Putra, M. H., Biswas, A. K., Behera, A. K., & Groβ, A. (2023). Insight on the choice of sensitizers/dyes for dye sensitized solar cells: A review. *Dyes and Pigments*, *213*, 111087.

Sharma, K., Sharma, V., & Sharma, S. S. (2018). Dye-Sensitized Solar Cells: Fundamentals and Current Status. *Nanoscale Research Letters*, *13*. https://doi.org/10.1186/s11671-018-2760-6

Soc, J. B. C., Costa, R. G. M., Farias, F. R. L., Maqueira, L., Neto, C. C., Carneiro, L. S. A., Almeida, J. M. S., Buarque, C. D., Aucélio, Q., & Limberger, J. (2019). Synthesis, Photophysical and Electrochemical Properties of Novel D-  $\pi$  -D and D-  $\pi$  -A Triphenylamino-Chalcones and  $\beta$  -Arylchalcones. 30(1), 81–89.

Tseng, C.-Y., Taufany, F., Nachimuthu, S., Jiang, J.-C., & Liaw, D.-J. (2014). Design strategies of metal free-organic sensitizers for dye sensitized solar cells: Role of donor and acceptor monomers. *Organic Electronics*, *15*(6), 1205–1214.

Unny, D., Sivanadanam, J., Mandal, S., Aidhen, I. S., & Ramanujam, K. (2018). Effect of Flexible, Rigid Planar and Non-Planar Donors on the Performance of Dye-Sensitized Solar Cells. *Journal of The Electrochemical Society*, *165*(13), H845–H860. https://doi.org/10.1149/2.0551813jes

Wan, Z., Jia, C., Duan, Y., Zhang, J., Lin, Y., & Shi, Y. (2012). Effects of different acceptors in phenothiazine-triphenylamine dyes on the optical, electrochemical, and photovoltaic properties. *Dyes and Pigments*, 94(1), 150–155. https://doi.org/https://doi.org/10.1016/j.dyepig.2011.12